sciendo

Research Article   **Open Access**

Nabil Manchar, Chaouki Benabbas, Riheb Hadji*, Foued Bouaicha, Florina Grecu

Landslide Susceptibility Assessment in Constantine Region (NE Algeria) By Means of Statistical Models

Abstract: The purpose of the present study was to compare the prediction performances of three statistical methods, namely, information value (IV), weight of evidence (WoE) and frequency ratio (FR), for landslide susceptibility mapping (LSM) at the east of Constantine region. A detailed landslide inventory of the study area with a total of 81 landslide locations was compiled from aerial photographs, satellite images and field surveys. This landslide inventory was randomly split into a testing dataset (70%) for training the models, and the remaining (30%) was used for validation purpose. Nine landslide-related factors such as slope gradient, slope aspect, elevation, distance to streams, lithology, distance to lineaments, precipitation, Normalized Difference Vegetation Index (NDVI) and stream density were used in the landslide susceptibility analyses. The inventory was adopted to analyse the spatial relationship between these landslide factors and landslide occurrences. Based on IV, WoE and FR approaches, three landslide susceptibility zonation maps were categorized, namely, "very high, high, moderate, low, and very low". The results were compared and validated by computing area under the receiver operating characteristic (ROC) curve (AUC). From the statistics, it is noted that prediction scores of the FR,

IV and WoE models are relatively similar with 73.32%, 73.95% and 79.07%, respectively. However, the map, obtained using the WoE technique, was experienced to be more suitable for the study area. Based on the results, the produced LSM can serve as a reference for planning and decision-making regarding the general use of the land.

Keywords: geographic information system; probabilistic methods; information value; weight of evidence; frequency ratio.

1 Introduction

Natural hazards comport all injurious geophysical events, such as earthquakes, flooding and landsliding [1-8]. Landslides occur worldwide; however, their frequency/intensity is greater in countries with mountainous and hilly environments [9, 10]. Only for earthquakes and movements of land, the NE of Algeria is yearly affected by loss of property greater than that caused by any other problem, especially in the Constantine province, where recurrent slope failures caused severe damages [11, 12]. To the east of the chief town, the A1 highway and its neighbouring have been affected by spectacular mass movements during and after its construction [13].

Landslide susceptibility assessment has become a major research topic in the last few decades [14]. It is often performed through the identification, analysis and combination of landslide causative factors. It is generally approached by two broad techniques: (i) qualitative approaches, based on expert knowledge, and (ii) quantitative approaches based on statistical analysis [15-19]. Nowadays, the quantitative approaches are the most used. They are based on mathematical expressions of the relationship between conditioning factors and the landslides, usually managed as thematic data within geographic information system (GIS). Their two main branches include deterministic methods, more appropriate for large scale [20], and statistical methods,

*Corresponding author: Riheb Hadji, Department of Earth Sciences, Institute of Architecture and Earth Sciences, Setif 1 University, Algeria, E-mail: hadjirihab@yahoo.fr
Nabil Manchar: Department of Geological Sciences, University of Frères Mentouri-Constantine 1, Postbox 325, Ain El Bey Street, 25017 Constantine, Algeria; Department of Geology, Larbi Ben M'Hidi University, Oum El Bouaghi 04000, Algeria
Chaouki Benabbas: Institute of Urban Technology Management, Constantine 3 University, Algeria
Foued Bouaicha: Department of applied biology, Université Frères Mentouri – Constantine 1 BP, 325 Route de Ain El Bey, Constantine, Algérie, 25017
Florina Grecu: Faculty of Geography, Geomorphology- Pedology-Geomatics DepartmentUniversity of Bucharest, Romania

valid for small and medium scale, such as weight of evidence (WoE), information value (IV), frequency ratio (FR), fuzzy logic (FL), logistic regression (LR) and artificial neural network (ANN) approaches [21, 22]. So far, there is no agreement that which one is the best, but the general consensus is that each method has its advantages and disadvantages [23, 24].

The aims of this study were to assess landslide susceptibility for the east of Constantine province, using the WoE, IV and FR models, and to measure their performances based on the receiver operating characteristic (ROC) analysis [25]. This information could be used by land planners to estimate the threats to population, property and transportation network.

The study area is located the east of the Constantine province (NE Algeria), known as one of the most landslide prone areas in NE of Algeria. It frames 6°37'30" to 6°49'30"longitude and, 36°16'30"to 36°27'35" latitude and spans on 351 km². The altitude of the landscape ranges from 500 m to 1200 m a.s.l. distinguishing several mountains such as Jebel Kellal (950 m), Jebel El Ouahche (1100 m) and Kef El Akahl (1200 m), culminating on Boumerzoug, Hamimin, El Aria and Ennaga wadies.

The study area is characterized by a complex morphology and a semi-arid climate with two typical rainy and dry seasons in contrast [26]. The precipitation ranges between 450 and 500 mm/year [27]. About 63% of the annual rainfall quantity is concentrated between December and February [28]. Geologically, the studied area is characterized by superposition of thrust sheet units made up from the base to the top by neritic unit (cretaceous carbonate); ultra-Tellian unit (cretaceous-eocene marls and marly limestone); Tellian *sensu-stricto* (*s.s.*): marly dominance (Cretaceous-Eocene); Numidian unit with sandstone Burdigalian, clay and flysch (Eocene) and Mio-Plio-Quaternary: sandy clays, marls and conglomerate (Mio-Pliocene) [47]. Alluvial terraces and lacustrine calcareous formations with the Quaternary age. This structure was deposited during the Eocene and Miocene paroxysmal compressional phases (Fig. 1).

2 Materials and Methodology

2.1 Landslide characteristics and inventory map

Preparing landslide maps is a preliminary step in landslide susceptibility assessment [29]. This allows to control the distribution, extent, types and patterns of landslides in relation to geomorphological, geological and environmental parameters [30]. The inventory map of the study area enumerates 81 slope failures (78 rotational slides, a planar slide, a solifluction and a debris flow) (Fig. 2a). It was carried out depending on the surveys conducted by the Algerian of Highways (ADA), as well as the visual interpretation of air photos and satellite images. During field studies, all landslides were checked and mapped with the aid of a global positioning system (GPS). The slope failures seem to be more frequent in the NE part of the study area, dominated by weak formations. In this research, the landslide inventory was randomly divided into 70% (57 events) for training the model and 30% (24 events) for its validation (Fig. 3) [21].

2.2 Conditioning factors related to landslides

The geoenvironmental characteristics of an area control the initiation of slope failures in many ways. They could be considered as conditioning factors in the phenomenon prediction. In our research, both predisposition and triggering factors were selected among those most commonly used in landslide susceptibility assessment [31]. The data source used in this study comes from Landsat 7 Enhanced Thematic Mapper Plus (ETM+) images, aerial photographs, geologic and topographic maps, etc. A contour map at 10 m intervals was digitized from (1/25000) topographic map and subsequently employed for generating a digital elevation model (DEM) of the study area. The related physiographic features were directly extracted from the DEM to construct the landslide susceptibility models.

2.2.1 Lithology

Geologic factors play an important role in slope failures and consequently in landslide susceptibility assessment [32]. The lithological map of the study area (Fig. 4a) was defined by the digitization of outcrop formation from "El Aria" geological map (No 74) published by the Algerian Geological Survey Agency (ASGA). The variability of the lithologies in the study area is classified into seven main lithological groups.

2.2.2 Slope gradient

The most important intrinsic factor influencing slope stability is the steepness of the slope [33]. The slopes in
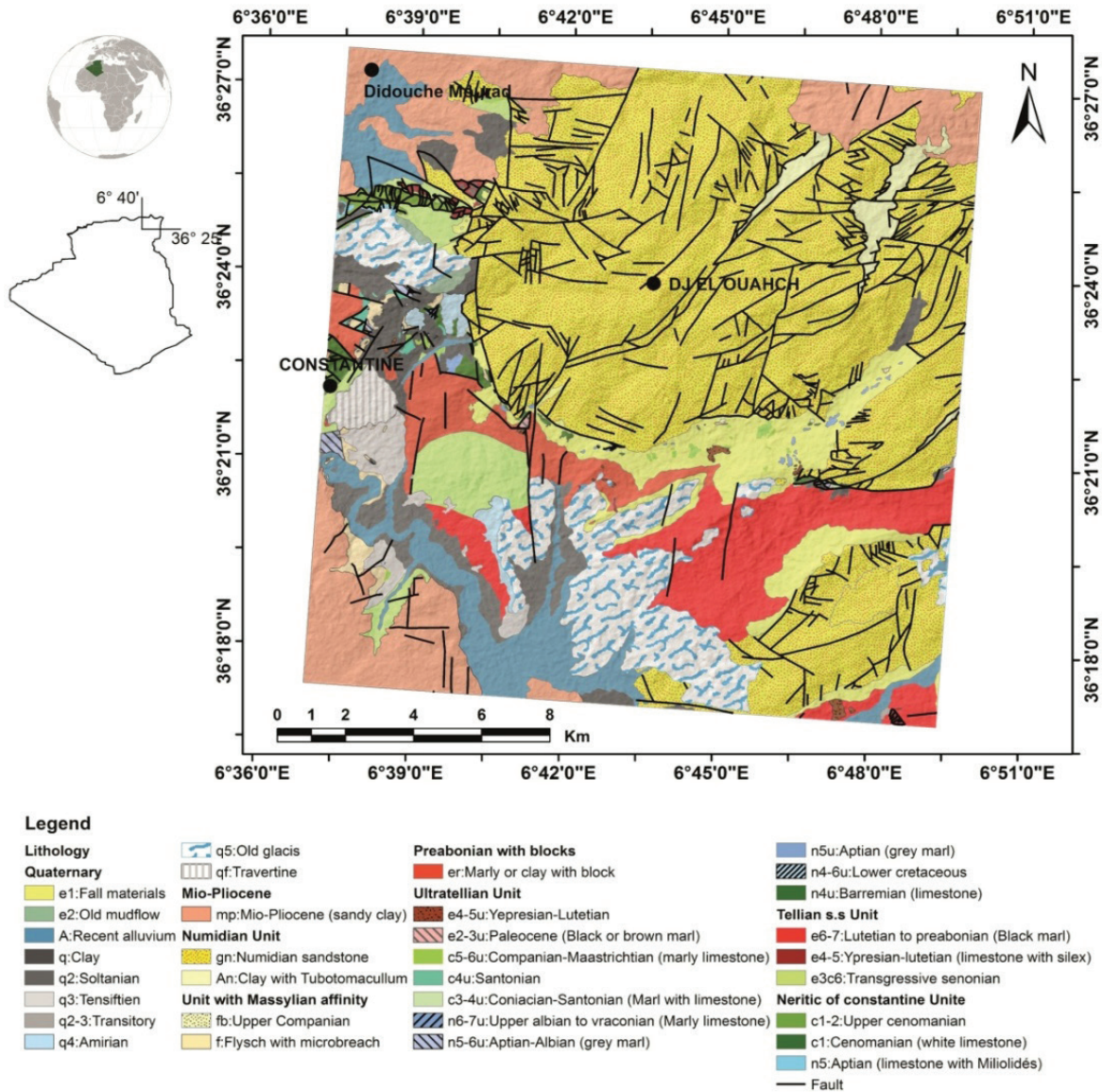
Legend

Lithology

Quaternary
- e1:Fall materials
- e2:Old mudflow
- A:Recent alluvium
- q:Clay
- q2:Soltanian
- q3:Tensiftien
- q2-3:Transitory
- q4:Amirian

- q5:Old glacis
- qf:Travertine

Mio-Pliocene
- mp:Mio-Pliocene (sandy clay)

Numidian Unit
- gn:Numidian sandstone
- An:Clay with Tubotomacullum

Unit with Massylian affinity
- fb:Upper Companian
- f:Flysch with microbreach

Preabonian with blocks
- er:Marly or clay with block

Ultratellian Unit
- e4-5u:Yepresian-Lutetian
- e2-3u:Paleocene (Black or brown marl)
- c5-6u:Companian-Maastrichtian (marly limestone)
- c4u:Santonian
- c3-4u:Coniacian-Santonian (Marl with limestone)
- n6-7u:Upper albian to vraconian (Marly limestone)
- n5-6u:Aptian-Albian (grey marl)

- n5u:Aptian (grey marl)
- n4-6u:Lower cretaceous
- n4u:Barremian (limestone)

Tellian s.s Unit
- e6-7:Lutetian to preabonian (Black marl)
- e4-5:Ypresian-lutetian (limestone with silex)
- e3c6:Transgressive senonian

Neritic of constantine Unite
- c1-2:Upper cenomanian
- c1:Cenomanian (white limestone)
- n5:Aptian (limestone with Miliolidés)

—— Fault

Figure 1: Geological map of the study area.

the study area were divided into seven categories based on an interval of 5° (Fig. 4b).

2.2.3 Slope aspect

The slope aspect usually plays a significant role in controlling some related climatic factors such as rain exposure, soil moisture and weathering [34]. The aspect map was classified into eight main classes, with the addition of flat lands (Fig. 4c).

2.2.4 Elevation

In many referential studies in landslide susceptibility, elevation was considered as an influential factor in slope stability [35]. The elevation in the study area was divided into seven categories based on an interval of 100 m (Fig. 4d).

2.2.5 Distance to lineaments

Lineaments play an important role in landslide initiation [36]. Based on digitized faults, folds, and fractures, the distance to lineaments map was classified into eight
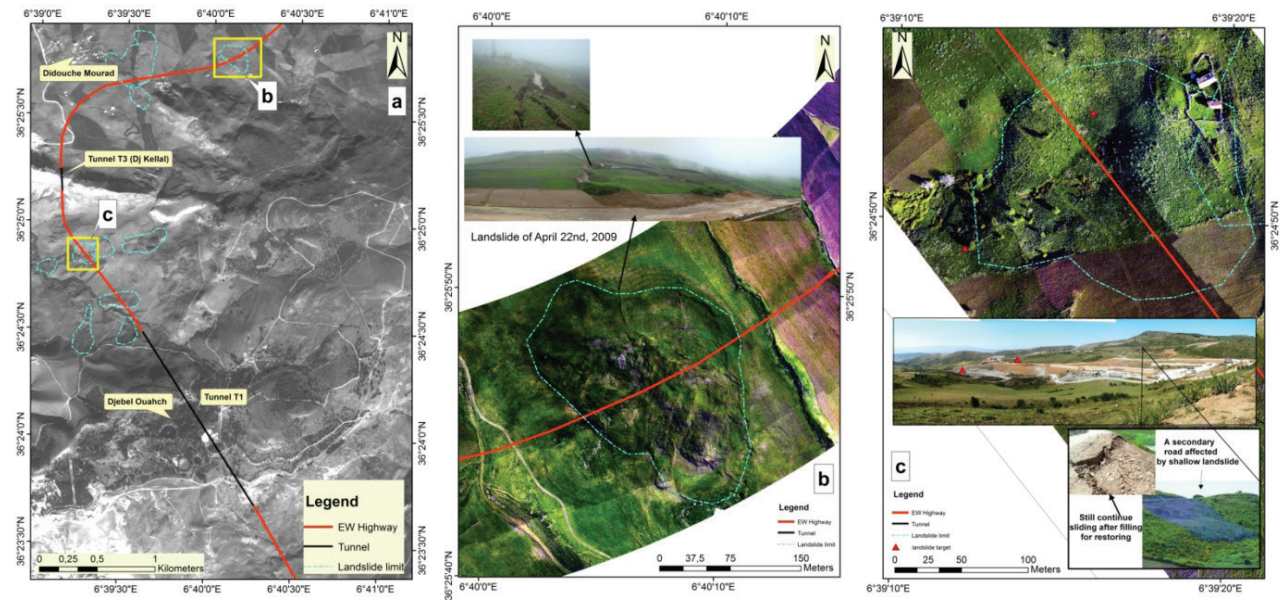
Figure 2: Optical remote sensing images and air photo used for the landslides determination in the study area: a- Panchromatic satellite image. b- A landslide occurred in highway's segment before construction (air photo). c- A neighboring road affected by a rotational landslide.
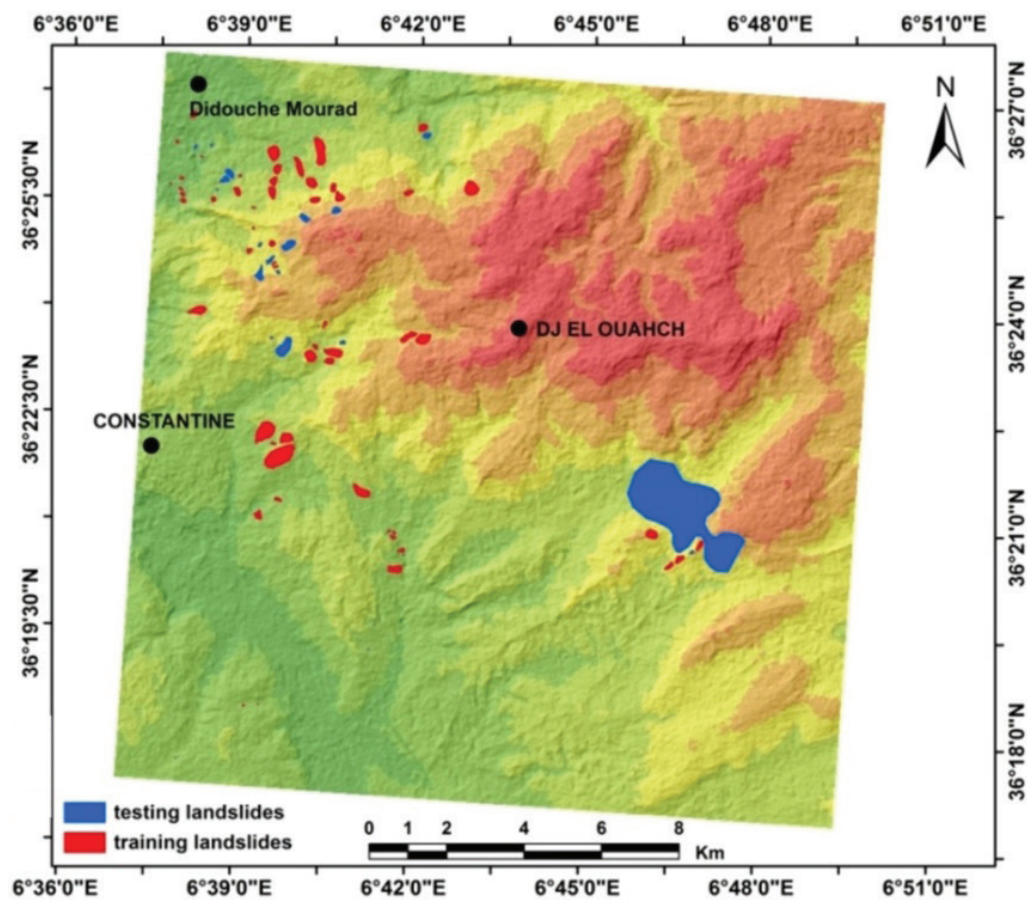

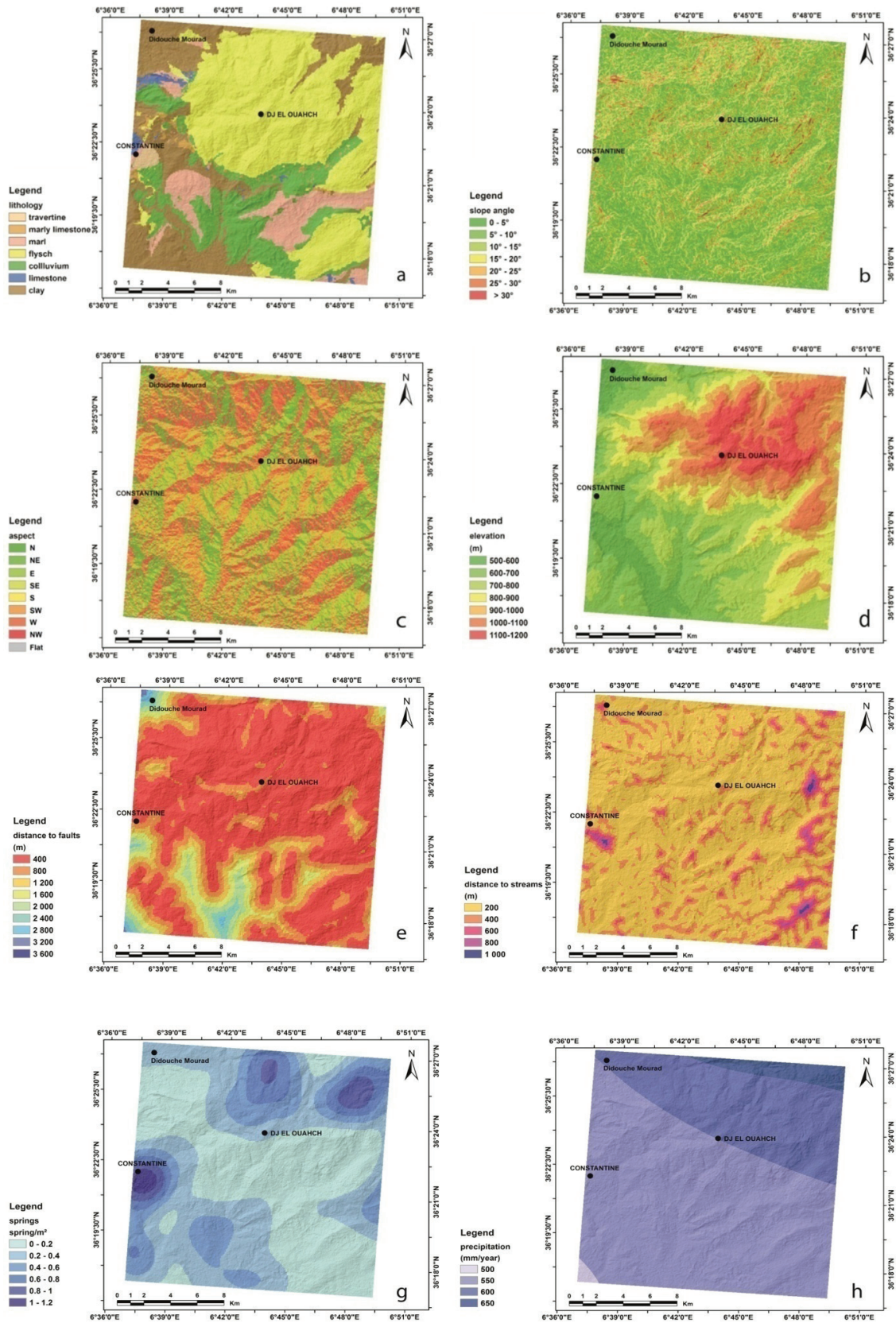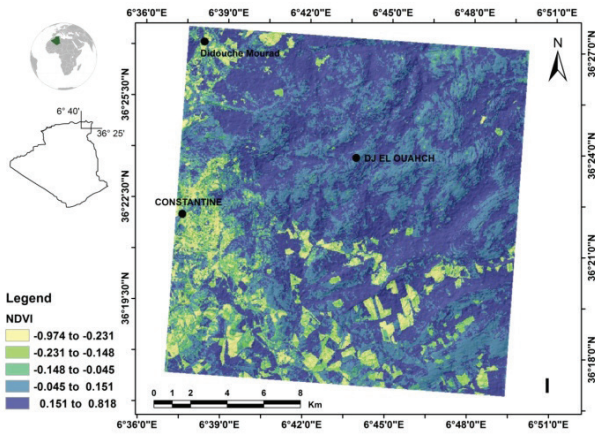**Figure 3:** Landslide inventory map of the study area.

Figure 4: Landslide conditioning factor used for landslide susceptibility mapping in the study area: a- Lithology. b- Slope angle. c- Slope aspect. d- Elevation.

Figure 4: Landslide conditioning factor used for landslide susceptibility mapping in the study area: a- Lithology. b- Slope angle. c- Slope aspect. d- Elevation.

lengths from 400 to 3200 m, at 400 m steps, with an additional ninth category for distances greater than 3400 m (Fig. 4e).

2.2.6 Distance to streams and stream density

The streams network is an important controlling factor of landslide occurrence [37], as its erosion action may undercut the foot of slopes [38]. The distance to the stream was classified into four lengths from 200 to 800 m, at 200 m steps, with an additional fifth category >1000 m (Fig. 4f). The map interpreting the Kernel density of streams was processed from the terrain hydrographic network features (Fig. 4g).

2.2.7 Rainfall

The most important triggering factor influencing the slope stability is the rainfall [39]. The annual average rainfall map was obtained from the inverse distance weight (IDW) interpolation of data from five hydroclimatic stations (Constantine, Hamma Bouziane, Aïn El Bey, Fourchi and Bir Drimil) over a 32-year period. The study areas get precipitations from 500 to 650 mm of rainfall (Fig. 4h).

2.2.8 Normalized Difference Vegetation Index (NDVI)

The NDVI is considered an influencing factor in landslide susceptibility assessment as it estimates the vegetation density [40]. The NDVI map (Fig. 4i) was calculated from Landsat 7 ETM+ scene by using a non-linear

transformation of the red and near-infrared bands of satellite images, using the following formula:

$$NDVI = (NIR - R)/(NIR + R) \tag{1}$$

where NIR and R are the reflectance in the near-infrared and red portions of the electromagnetic spectrum, respectively.

2.3 Methodology

In this research, landslide susceptibility mappings (LSMs) were designed by means of landslide inventory and FR, WoE and IV techniques. In order to evaluate the consistency of the three models, area under the ROC curve (AUC) was plotted using the Microsoft Excel software [41]. This method is commonly used to measure how much the model was successful in modelling and predicting the results. All LSMs were classified into five landslide susceptibility classes using Natural Breaks (NB) classifier [14].

2.3.1 Weight of evidence

The WoE is a statistical technique for landslide susceptibility assessment that uses landslide occurrence as training points to derive prediction outputs [42]. This method uses the log-linear from the Bayesian probability model in order to estimate the relative importance of evidence by a statistical mean, as given in the following equation [43].

$$P(A|B) = P(B|A) * \frac{P(A)}{P(B)} \tag{2}$$

Based on the presence or absence of the landslide within the area (A), this method calculates the weight for each landslide predictive factor (B) [44], and it is written as

$$Wi^+ = \ln\left(\frac{P\{B|A\}}{P\{B|\overline{A}\}}\right) \tag{3}$$

$$Wi^- = \ln\left(\frac{P\{\overline{B}|A\}}{P\{\overline{B}|\overline{A}\}}\right) \tag{4}$$

where P is the probability, B is the presence of potential landslide predictive factor, $\overline{B}$ is the absence of potential landslide predictive factor and A is the presence and $\overline{A}$ is the absence of landslides. Positive (W^+) and negative (W^-) weights indicate the correlation between the presence of

the causative factor and landslides. The contrast weight is the difference between the W^+ and W^- ($C = W^+ - W^-$); the C factor reflects the total spatial correlation between landslides and the desired causative factor.

2.3.2 Information value

The IV is a very useful concept for variable selection during model building [45]. In this method, the weight for factor class is defined as the natural logarithm of the landslide density in the class divided by the density of landslide in total area. The formula for IV is shown in the following [46]:

$$S_{if} = \ln\left(\frac{D_{if}}{D}\right) = \ln\left[\left(\frac{N_{if}}{P_{if}} \bigg/ \frac{N}{P}\right)\right] \qquad (5)$$

where S_{if} is the weight given to a given class i of the factor f, D_{if} is the landslide density inside the class i of the factor f, D is the landslide density inside the total area, N_{if} is the number of landslides in a given class i of the parameter f, P_{if} is the number of pixels in class i of the factor f, N is the total landslides within the study area and P is the total pixels inside the study area.

2.3.3 Frequency ratio

The FR is a useful method for variable integration while developing LSM [9]. It permits the derivation of spatial relationships between the landslide distribution and each causative factor. The FR is the ratio between landslides in factor class and the percentage of the area in the same class. The LSM is calculated by a summation of all factor ratios.

$$\text{LSM} = \sum_{i=1}^{n} \text{FR}_i \qquad (6)$$

3 Result and Validation

3.1 Spatial relationship between causative factors and landslides

The resulted IV, WoE and FR susceptibility maps show close similarities between overall the three methods. The conditioning factors were classified into classes, and weights are presented in columns 7, 10 and 13 of Table 1.

According to Table 1, the relation between landslides and slope gradient shows that most of the landslides were observed for slopes >30°. This means that there exists a good correlation between slope angle and the occurrence of landslides. Counter to the slope, there is no specific correlation between the elevation and the occurrence of landslides. For the slope aspect, the most susceptible classes are N and SW. Regarding the stream density factor, the most suitable class is 0.8–1. In the case of NDVI factor, the susceptibility increases gradually with the decrease in NDVI values. The relation between the lithology and landslide inventory of the study area shows that landslides occurred mainly in (i) Mio-Pliocene and Numidian clay, marl of the Tellian unit and clayey marl of Priabonian, current superficial deposits and colluvium and (ii) the flysh of Numidian unit. Concerning rainfall factor, the classes greater than 550 mm are the most susceptibles. The relation between landslide occurrences and distance to lineaments and streams shows that a large number of the landslides were observed in the area with a distance less than 400 m and 200 m, respectively.

3.2 Landslide susceptibility mapping

The produced LSMs of the three methods (Fig. 5a−c) were subdivided into five hierarchic classes (very low, low, moderate, high and very high) using the NB classifier. The very high susceptibility zones are located in the NW and SE of the study area spreading out 22% (IV), 19% (WoE) and 9% (FR) of the total area. The moderate susceptibility has a close distribution with 21.59% (IV), 25.17% (WoE) and 29.49% (FR) of the total area. Finally, the low to very low susceptibility is spread in the N, NE and SW of the study area within the average of 24.1% (IV), 27% (WoE) and 39.35% (FR).

In order to verify quantitatively the consistency of the models, the landslide density (LD) for each class was calculated. The LD values reach 3.09 (IV), 3.35 (FR) and 3.38 (WoE) in very high and high susceptibility zones. This confirms the proneness to landsliding in these areas when compared to those of moderate, low and very low susceptibility. The very low susceptible area has the lowest values of LD with 0.0323 (IV), 0.04 (FR) and 0.02 (WoE). According to Table 2, it can be explained that there is a gradual decrease in LD from the high to the low susceptible area.

Table 1: Spatial relationship between landslide and conditioning factors in the study.

Factor	Classes	Landslide pixels in classes	IV (S_{if})	D_{if}	(D)	FR % of total area (a)	% of landslide area (b)	FR	WoE W+	W-	C
Lithology	Flysch	8395	-0.343	-28.61	83.5	45.52	32.31	0.71	-0.357	0.383	-0.740
	Clay	7450	0.175	14.61		24.07	28.67	1.19	0.184	1.096	-0.911
	Marl	5188	0.710	59.29		9.81	19.97	2.03	0.762	2.150	-1.388
	Colluvium	4950	0.075	6.22		17.68	19.05	1.08	0.078	1.525	-1.447
	Marly limestone	0	0.000	0.00		1.09	0.00	0	–	–	–
	Limestone	0	0.000	0.00		1.13	0.00	0	–	–	–
	Travertine	0	0.000	0.00		0.70	0.00	0	–	–	–
Slope gradient (°)	0–5°	504	-3.156	-315.63	100.0	45.52	1.94	0.04	-3.202	0.722	-3.924
	5–10°	7603	0.195	19.54		24.07	29.26	1.22	0.206	1.089	-0.883
	10–15°	9870	1.354	135.37		9.81	37.99	3.87	1.503	1.993	-0.490
	15–20°	4504	-0.020	-1.99		17.68	17.33	0.98	-0.021	1.541	-1.562
	20–25°	2207	2.053	205.31		1.09	8.49	7.79	2.451	4.829	-2.377
	25–30°	678	0.842	84.15		1.13	2.61	2.32	0.908	4.527	-3.619
	>30°	618	1.219	121.93		0.70	2.38	3.38	1.342	5.057	-3.715
Rainfall (mm)	500	0	0.000	0.00	74.6	0.51	0.00	0	-	-	-
	550	22019	0.226	16.86		67.60	84.74	1.25	0.238	-1.476	1.715
	600	3964	-0.606	-45.25		27.98	15.26	0.55	-0.628	1.086	-1.715
	650	0	0.000	0.00		3.91	0.00	0	–	–	–
Distance to lineaments (m)	0–400	17409	0.070	7.04	100.0	62.44	67.00	1.07	0.074	-0.634	0.708
	400–800	8377	0.491	49.06		19.74	32.24	1.63	0.522	1.264	-0.743
	800–1200	22	-4.670	-466.96		8.89	0.08	0.01	-4.716	2.372	-7.089
	1200–1600	88	-2.616	-261.55		4.63	0.34	0.07	-2.659	3.025	-5.684
	1600–2000	88	-2.085	-208.52		2.73	0.34	0.12	-2.127	3.558	-5.684
	2000–2400	0	0.000	0.00		1.15	0.00	0	–	–	–
	2400–2800	0	0.000	0.00		0.34	0.00	0	–	–	–
	2800–3200	0	0.000	0.00		0.08	0.00	0	–	–	–
	3200–3600	0	0.000	0.00		0.00	0.00	0	–	–	–
Distance to streams (m)	0–200	23041	0.183	13.57	74.2	73.86	88.68	1.20	0.193	-1.866	2.058
	200–400	2942	-0.612	-45.38		20.87	11.32	0.54	-0.634	1.425	-2.058
	400–600	0	0.000	0.00		4.12	0.00	0	-	–	–
	600–800	0	0.000	0.00		0.98	0.00	0	–	–	–
	800–1000	0	0.000	0.00		0.17	0.00	0	–	–	–
Elevation (m)	500–600	1347	-0.424	-25.07	59.2	7.92	5.19	0.65	-0.440	2.466	-2.906
	600–700	3040	-0.520	-30.78		19.68	11.70	0.59	-0.540	1.481	-2.021
	700–800	8249	0.422	24.99		20.81	31.75	1.53	0.448	1.214	-0.765
	800–900	8607	0.811	47.96		14.73	33.12	2.25	0.873	1.575	-0.703
	900–1000	4453	0.160	9.48		14.60	17.14	1.17	0.169	1.745	-1.576
	1000–1100	288	-2.576	-152.40		14.55	1.11	0.08	-2.620	1.872	-4.492
	1100–1200	0	0.000	0.00		7.71	0.00	0	–	–	–
NDVI	-0.974–0.231	61	-3.216	-35.11	10.9	5.88	0.24	0.04	-3.261	2.785	-6.047
	0.231–0.148	154	-3.861	-42.15		28.13	0.59	0.02	-3.907	1.216	-5.123
	0.148–0.045	508	-1.110	-12.11		5.93	1.96	0.33	-1.141	2.774	-3.915
	0.045–0.151	2932	0.057	0.62		10.66	11.28	1.06	0.059	2.122	-2.062
	0.151–0.818	22328	0.554	6.05		49.40	85.93	1.74	0.590	-1.220	1.810

Continued **Table 1:** Spatial relationship between landslide and conditioning factors in the study.

| Factor	Classes	Landslide pixels in classes	IV			FR			WoE		
			(S_{if})	D_{if}	(D)	% of total area (a)	% of landslide area (b)	FR	$W+$	$W-$	C
Stream density	0–0.2	20887	0.616	33.22	53.9	1.85	80.39	1.85	0.658	-0.752	1.411
	0.2–0.4	3478	-0.851	-45.91		0.43	13.39	0.43	-0.879	0.988	-1.867
	0.4–0.6	492	-2.057	-110.92		0.13	1.89	0.13	-2.099	1.850	-3.948
	0.6–0.8	1126	-0.426	-22.99		0.65	4.33	0.65	-0.443	2.651	-3.094
	0.8–1	0	0.000	0.00		0.00	0.00	0	–	–	–
	1–1.2	0	0.000	0.00		0.00	0.00	0	–	–	–
Slope aspect	N	7306	0.922	65.77	71.3	11.18	28.12	2.51	0.998	1.937	-0.939
	NE	2162	-0.157	-11.23		9.74	8.32	0.85	-0.165	2.235	-2.399
	E	2763	-0.092	-6.55		11.66	10.64	0.91	-0.096	2.032	-2.129
	SE	1622	-0.760	-54.21		13.35	6.24	0.47	-0.786	1.924	-2.709
	S	2380	-0.408	-29.09		13.77	9.16	0.67	-0.424	1.870	-2.294
	SW	4074	0.173	12.35		13.19	15.68	1.19	0.182	1.865	-1.682
	W	2938	-0.225	-16.07		14.16	11.31	0.80	-0.235	1.825	-2.060
	NW	2738	-0.206	-14.68		12.95	10.54	0.81	-0.215	1.924	-2.139
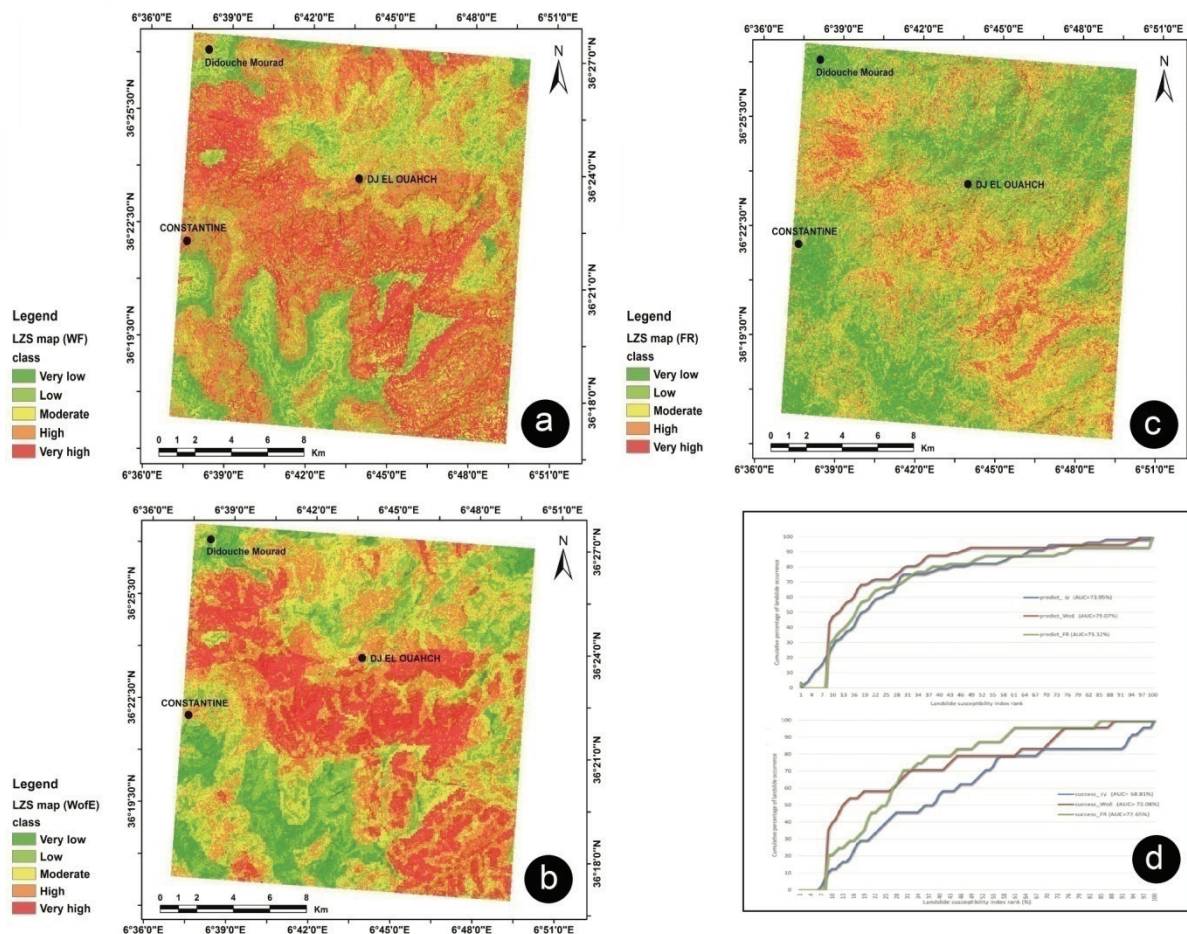
Figure 5: LSMs for a: IV, b: WoE, and c: FR. d: ROC curves of the three used models.

Table 2: LD in different susceptibility zones of the study area (IV, WoE, FR)..

Susceptibility	Area		Landslide area		LD
	km²	%	km²	%	
IV					
Very low	14.817	6.58	0.015	0.21	0.0323
Low	39.457	17.52	0.124	1.72	0.0981
Moderate	48.609	21.59	0.626	8.65	0.4007
High	72.912	32.38	1.553	21.46	0.6627
Very high	49.362	21.92	4.917	67.96	3.0998
FR					
Very low	27.481	12.21	0.032	0.44	0.0363
Low	61.116	27.14	0.602	8.33	0.3068
Moderate	66.398	29.49	0.735	10.16	0.3446
High	49.896	22.16	5.372	74.25	3.3504
Very high	20.266	9.00	0.493	6.82	0.7577
WoE					
Very low	19.669	8.74	0.015	0.21	0.0243
Low	41.123	18.26	0.097	1.33	0.0730
Moderate	56.676	25.17	0.393	5.43	0.2158
High	63.927	28.39	1.972	27.26	0.9602
Very high	43.762	19.44	4.758	65.76	3.3834

3.3 Validation procedure

In order to test the compatibility of the models and to determine their prediction ability, the AUC (success and prediction rates) was plotted. The prediction rates of the FR and WoE methods are in the range of 0.7332–0.7907, indicating a good performance of the models, with a slight differentiation for the WoE model. In the case of the success rates, the IV method shows a low score of 0.5881. This value is less convincing than the two remaining models (Fig. 5d).

3.4 Discussion

From these calculations, we can say that the slope gradient is the most important parameter for slope stability analysis, because the driving force of mass movement increases with increasing slope. In the study area, the gradients over than 25° in soft rocks and/or soils are the most susceptible to landsliding. Because of their physical behaviour, the clay, marl and colluvium formations are more prone to shear stress and therefore most susceptible to landslide occurrence. It is clear that elevation factor influences less the landslide occurrence, against to other factors. This is probably due to the accumulation of weathered materials on low altitudes (corresponding to gentle slopes) and hardness of outcropping formations in high altitudes. The streams network is a further controlling parameters of landslide occurrence, as streams' erosion may undercut the foot of the slopes and saturate their lower part. Moreover, for the fault proximity, we cannot extract a clear correlation between the nearness to faults and the landslide occurrence. The relation between landslide occurrence and NDVI shows that most of the landslides occur in areas with low values. The relation between aspect and landslide occurrences shows that most of the landslides were observed in areas with N and SW-facing slopes. This is probably due to the more exposure to rainfall coming from these sides.

4 Conclusions

In the last few years, many qualitative and quantitative methods have proved their worth in landslide susceptibility assessment. In this study, three statistical approaches were proposed to promote the advantages and overcome the shortcomings of GIS-based methods in assessing the susceptibility of landslides in the east of Constantine province, constantly threatened by this phenomenon. IV, WoE and FR are efficiently used to analyse the correlation between landslide occurrence and their conditioning factors. Initially, a single event-based landslide inventory was established and was then randomly divided into training and validation datasets. Nine causative factors were adopted for the landslide susceptibility analysis such as slope gradient, slope aspect, elevation, distance to streams, lithology, distance to lineaments, precipitation, NDVI and stream density. Weights and class indexes were attributed to each of the associated factors. The three LSMs were categorized: namely, "very high, high, moderate, low, and very low" using NB classifier. The resulted maps have been validated by comparison with known landslide locations. The WoE presents the higher prediction rate (79.07%), distinguished as the most performant model for the landslide susceptibility assessment in the study area. The results show that the slope gradient, rainfall, lithology and distance to streams are the most influencing factors in landslide occurrence according to their associated weights. The obtained LSMs provide helpful tools for the decision-makers and engineers. They may assist as good beneficial guides for planners in the scope of choosing appropriate locations for the implementation of developments.

References

[1] Pradhan, B. (2013). A comparative study on the predictive ability of the decision tree, support vector machine and NF models in landslide susceptibility mapping using GIS. *Computers & Geosciences*, *51*, 350-365.

[2] Van Westen, C.J. (2013). Remote sensing and GIS for natural hazards assessment and disaster risk management. In *Treatise on Geomorphology*, Edited by: Shroder, J., Bishop, MP, Academic Press, San Diego, CA, *3*, 259-298.

[3] Park, S., Choi, C., Kim, B., Kim, J. (2013). Landslide susceptibility mapping using frequency ratio, analytic hierarchy process, logistic regression, and artificial neural network methods at the Inje area, Korea. *Environmental Earth Sciences*, *68*(5), 1443-1464.

[4] Gadri, L., Hadji, R., Zahri, F., Benghazi, Z., Boumezbeur, A., Laid, B.M., et al. (2015). The quarries edges stability in opencast mines: a case study of the Jebel Onk phosphate mine, NE Algeria. *Arabian Journal of Geosciences*, *8*(11), 8987-8997.

[5] Zahri, F., Boukelloul, M.L., Hadji, R., Talhi, K. (2016). Slope stability analysis in open pit mines of Jebel Gustar career, NE Algeria–a multi-steps approach. *Mining Science*, 23, 137-146.

[6] Mokadem, N., Demdoum, A., Hamed, Y., Bouri, S., Hadji, R., Boyce, A., et al. (2016). Hydrogeochemical and stable isotope data of groundwater of a multi-aquifer system: Northern Gafsa basin–Central Tunisia. *Journal of African Earth Sciences*, *114*, 174-191.

[7] Mouici, R., Baali, F., Hadji, R., Boubaya, D., Audra, P., Fehdi, C., et al. (2017). Geophysical, geotechnical, and speleologic assessment for karst-sinkhole collapse genesis in cheria plateau (NE Algeria). *Mining Science*, 24.

[8] Hamed, Y., Redhaounia, B., Ben Sâad, A., Hadji, R., Zahri, F. (2017). Groundwater inrush caused by the fault reactivation and the climate impact in the mining Gafsa basin (southwestern Tunisia). Journal of Tethys, 5(2), 154-164.

[9] Lee, S, and Pradhan, B. (2006). Probabilistic landslide hazard and risk mapping on Penang Island, Malaysia. *Journal of Earth System Science*, *115*, 661-672.

[10] Hadji, R., Chouabi, A., Gadri, L., Raïs, K., Hamed, Y., Boumazbeur, A. (2016). Application of linear indexing model and GIS techniques for the slope movement susceptibility modeling in Bousselam upstream basin, Northeast Algeria. *Arabian Journal of Geosciences*, *9*(3), 192.

[11] Bougdal, R., Belhai, D., Antoine, P. (2007). Géologie détaillée de la ville de Constantine et ses alentours: une donnée de base pour l'étude des glissements de terrain. *Bull ServGéol de l'Algérie*, *18*(2), 161–187.

[12] Bourenane, H., Guettouche, M., Bouhadad, Y. and Braham, M. (2016). Landslide hazard mapping in the Constantine city, Northeast Algeria using frequency ratio, information value, logistic regression, weights of evidence, and analytical hierarchy process methods. *Arabian Journal of Geosciences*, *9*(2).

[13] Achour, Y., Boumezbeur, A., Hadji, R., Chouabbi, A., Cavaleiro, V., Bendaoud, E.A. (2017). Landslide susceptibility mapping using analytic hierarchy process and information value methods along a highway road section in Constantine, Algeria. *Arabian Journal of Geosciences*, *10*(8), 194.

[14] Hadji, R., Achour, Y., Hamed, Y. (2017). Using GIS and RS for slope movement susceptibility mapping: comparing AHP, LI and LR methods for the Oued Mellah Basin, NE Algeria. In *Euro-Mediterranean Conference for Environmental Integration*. Springer, Cham, pp. 1853-1856.

[15] Carrara, A., Cardinali, M., Guzzetti, F., Reichenbach, P. (1995). GIS technology in mapping landslide hazard. In *Geographical Information Systems in Assessing Natural Hazards*. Edited by A. Carrara, F. Guzzetti. Springer, Dordrecht, pp. 135-175.

[16] Soeters, R., van Westen, C.J. (1996). Landslides: Investigation and mitigation. Chapter 8-Slope instability recognition, analysis, and zonation. Transportation Research Board Special Report, (247).

[17] Guzzetti, F., Carrara, A., Cardinali, M., Reichenbach, P. (1999). Landslide hazard evaluation: a review of current techniques and their application in a multi-scale study, Central Italy. *Geomorphology*, *31*(1), 181-216.

[18] Sharma, V.K. (2006). Landslide hazard zonation: an overview of emerging techniques. *Journal of Engineering Geology*, *XXXIII*, 73-80.

[19] Dahoua, L., Yakovitch, S.V., Hadji, R.H. (2017). GIS-based technic for roadside-slope stability assessment: An bivariate approach for A1 East-West highway, North Algeria. *Mining Science*, *24*, 117-127.

[20] Bourenane, H., Bouhadad, Y., Guettouche, M., Braham, M. (2014). GIS-based landslide susceptibility zonation using bivariate statistical and expert approaches in the city of Constantine (Northeast Algeria). *Bulletin of Engineering Geology and the Environment*, *74*(2), 337-355.

[21] Pradhan, B., Lee, S. (2010). Delineation of landslide hazard areas on Penang Island, Malaysia, by using frequency ratio, logistic regression, and artificial neural network models. *Environmental Earth Sciences*, *60*(5), 1037-1054.

[22] Yalcin, A., Reis, S., Aydinoglu, A.C., Yomralioglu, T. (2011). A GIS-based comparative study of frequency ratio, analytical hierarchy process, bivariate statistics and logistics regression methods for landslide susceptibility mapping in Trabzon, NE Turkey. *Catena*, *85*(3), 274-287.

[23] Karim, Z., Hadji, R., Hamed, Y. (2018). GIS-based approaches for the landslide susceptibility prediction in Setif Region (NE Algeria). *Geotechnical and Geological Engineering*, 1-16.

[24] Mahdadi, F., Boumezbeur, A., Hadji, R., Kanungo, D. P., Zahri, F. (2018). GIS-based landslide susceptibility assessment using statistical models: a case study from Souk Ahras province, NE Algeria. *Arabian Journal of Geosciences*, *11*(17), 476.

[25] Hadji, R., Limani, Y., Demdoum, A. (2014). Using multivariate approach and GIS applications to predict slope instability hazard case study of Machrouha municipality, NE Algeria. In *Information and Communication Technologies for Disaster Management (ICT-DM), 2014 1st International Conference on* IEEE, pp. 1-10.

[26] Hamad, A., Baali, F., Hadji, R., Zerrouki, H., Besser, H., Mokadem, N., et al. (2018). Hydrogeochemical characterization of water mineralization in Tebessa-Kasserine karst system (Tuniso-Algerian Transboundry basin). *Euro-Mediterranean Journal for Environmental Integration*, *3*(1), 7.

[27] Demdoum, A., Hamed, Y., Feki, M., Hadji, R., Djebbar, M. (2015). Multi-tracer investigation of groundwater in El Eulma Basin (northwestern Algeria), North Africa. *Arabian Journal of Geosciences*, *8*(5), 3321-3333.

[28] Hamed, Y., Ahmadi, R., Hadji, R., Mokadem, N., Dhia, H. B., Ali, W. (2014). Groundwater evolution of the continental intercalaire aquifer of Southern Tunisia and a part of Southern Algeria: Use of geochemical and isotopic indicators. *Desalination and Water Treatment*, *52*(10-12), 1990-1996.

[29] Yilmaz, I. (2009). Landslide susceptibility mapping using frequency ratio, logistic regression, artificial neural networks and their comparison: A case study from Kat landslides (Tokat—Turkey). *Computers & Geosciences*, *35*(6), 1125-1138.

[30] Tseng, C.M., Lin, C.W., Hsieh, W.D. (2015). Landslide susceptibility analysis by means of event-based multi-temporal landslide inventories. *Natural Hazards & Earth System Sciences Discussions*, *3*(2), 1137-1173.

[31] Hadji, R., Rais, K., Gadri, L., Chouabi, A., Hamed, Y. (2017). Slope failure characteristics and slope movement susceptibility assessment using GIS in a medium scale: a case study from Ouled Driss and Machroha municipalities, Northeast Algeria. *Arabian Journal for Science and Engineering*, *42*(1), 281-300.

[32] Hadji, R., Limani, Y., Boumazbeur, A.E., Demdoum, A., Zighmi, K., Zahri, F., et al. (2014). Climate change and its influence on shrinkage–swelling clays susceptibility in a semi-arid zone: a case study of Souk Ahras municipality, NE-Algeria. *Desalination and Water Treatment*, *52*(10-12), 2057-2072.

[33] Hadji, R., Boumazbeur, A., Limani, Y., Baghem, M., el Madjid Chouabi, A., Demdoum, A. (2013). Geologic, topographic and climatic controls in landslide hazard assessment using GIS modeling: a case study of Souk Ahras region, NE Algeria. *Quaternary International*, *302*, 224-237.

[34] Hamed, Y., Redhaounia, B., Sâad, A., Hadji, R., Zahri, F., Zighmi, K. (2017). Hydrothermal waters from karst aquifer: Case study of the Trozza basin (Central Tunisia). *Journal of Tethys*, *5*(1), 33-44.

[35] Guzzetti, F., Reichenbach, P., Cardinali, M., Galli, M. and Ardizzone, F. (2005). Probabilistic landslide hazard assessment at the basin scale. *Geomorphology*, *72*(1-4), 272-299.

[36] El Mekki, A., Hadji, R., Fehdi, C. (2018) Use of slope failures inventory and climatic data for landslide susceptibility, vulnerability, and risk mapping in Souk Ahras region. *Mining Science*, *24*, 237-249

[37] Besser, H., Mokadem, N., Redhaounia, B., Hadji, R., Hamad, A., Hamed, Y. (2018). Groundwater mixing and geochemical assessment of low-enthalpy resources in the geothermal field of southwestern Tunisia. *Euro-Mediterranean Journal for Environmental Integration*, *3*(1), 16.

[38] Dahoua, L., Yakovitch, S.V., Hadji, R., Farid, Z. (2017). Landslide susceptibility mapping using analytic hierarchy process method in BBA-Bouira Region, case study of east-west highway, NE Algeria. In *Euro-Mediterranean Conference for Environmental Integration*. Springer, Cham, pp. 1837-1840.

[39] Hamad, A., Hadji, R., Bâali, F., Houda, B., Redhaounia, B., Zighmi, K., et al., (2018). Conceptual model for karstic aquifers by combined analysis of GIS, chemical, thermal, and isotopic tools in Tuniso-Algerian transboundary basin. *Arabian Journal of Geosciences*, *11*(15), 409.

[40] Althuwaynee, O.F., Pradhan, B., Lee, S. (2012). Application of an evidential belief function model in landslide susceptibility mapping. *Computers & Geosciences*, *44*, 120-135.

[41] Lee, S. (2005). Application of logistic regression model and its validation for landslide susceptibility mapping using GIS and remote sensing data. *International Journal of Remote Sensing*, *7*, 1477-1491.

[42] Pardeshi, S.D., Autade, S.E., Pardeshi, S.S. (2013). Landslide hazard assessment: recent trends and techniques, *Springer Plus*, *2*, 253.

[43] Pradhan, B., Oh, H.J., Buchroithner, M. (2010). Weights-of-evidence model applied to landslide susceptibility mapping in a tropical hilly area. *Geomatics, Natural Hazards and Risk*, *1*(3), 199-223.

[44] Lee, S., Choi, J., Min, K., (2004). Probabilistic landslide hazard mapping using GIS and remote sensing data at Boun, Korea. *International Journal of Remote Sensing*, *25*(11), 2037-2052.

[45] Cevik, E., Topal, T. (2003). GIS-based landslide susceptibility mapping for a problematic segment of the natural gas pipeline, Hendek (Turkey). *Environmental Geology*, *44*(8), 949-962.

[46] Van Westen, C.J. (1993). Application of geographic information systems to landslide hazard zonation. ITC Publication, vol. 15. International Institute for Aerospace and Earth Resources Survey, Enschede, p. 245.

[47] Hamed, Y., Hadji, R., Redhaounia, B., Zighmi, K., Bâali, F., El Gayar, A. (2018). Climate impact on surface and groundwater in North Africa: a global synthesis of findings and recommendations. *Euro-Mediterranean Journal for Environmental Integration*, *3*(1), 25.